

FUSE Observations of Stellar Winds in Early LMC O Stars

D. Massa (Raytheon ITSS) and A.W. Fullerton (UVic and JHU)

We present *FUSE* observations of 13 LMC O3-7 stars. The wind lines in the *FUSE* range and those with *HST* or high resolution *IUE* data were analyzed using a Sobolev with Exact Integration (SEI) model.

The Sample

- ▶ Thirteen early LMC O stars listed in Table 1.
- ▶ So far, only resonance lines have been analyzed.

SEI Modelling

- ▶ Used a β velocity law, a single turbulent velocity and a completely flexible τ_{rad} – Figure 1.
- ▶ A model of the ISM H and H₂ opacity was also required to interpret the observations.

Results

- ▶ Figure 2 shows the ion fractions, q_i , as a function of $w = v/v_\infty$ for each star.
- ▶ Table 2 lists the mean ion fractions ($\langle q_i \rangle = \int_{0.2}^{0.9} q_i dw / \int_{0.2}^{0.9} dw$) for the wind lines analyzed.
- ▶ Figure 3 shows examples of ionic ratios, which are independent of \dot{M} estimates.

Discussion

- ▶ In general, the ionization state of the wind decreases as w increases.
- ▶ $\langle q(\text{P v}) \rangle$ can exceed 10% and avoid saturation because of P's low intrinsic abundance. It appears that P v is often the *dominant ion* of Phosphorus in the wind.
- ▶ $\langle q(\text{O IV}) \rangle$ correlates with v_∞ – possibly indicating a shock strength dependence (Fig. 4).
- ▶ $\langle q(\text{S VI}) \rangle$ is negatively correlated with luminosity (Fig. 4).
- ▶ On the basis of a comparison of with Sk-67°167, it appears that Sk-67°166 is an ON star.

FUSE is operated for NASA by the Johns Hopkins University under NASA contract NAS5-32985.

Table 1: LMC Early O Stars

Sanduleak	Spectral Type	v_∞ (km s ⁻¹)	$\log L/L_\odot^{(1)}$	$T_{eff}^{(2)}$	R/R _⊙	$\dot{M}^{(3)}$ (M/M _⊙ yr ⁻¹)
-67° 211	O3 III(f*)	3600	6.18	50960	16.4	1.00×10^{-5}
-66° 172	O3 III(f*)+OB	3100	5.92	50960	12.2	4.53×10^{-6}
-67° 166	O4 If+	1825	6.18	47690	18.7	1.88×10^{-5}
-67° 167	O4 Inf+	2000	6.11	47690	17.3	1.31×10^{-5}
-70° 115	O4 III(f)	2200	6.46	48180	25.3	4.28×10^{-5}
-71° 45	O4-5 III(f)	2500	6.60	46800	31.5	6.09×10^{-5}
-70° 60	O5 V((f))/O4 V	2500	5.49	47400	8.6	1.10×10^{-6}
-70° 69	O5 V	3000	5.25	46120	6.9	3.73×10^{-7}
-65° 22	O6 Iaf+	1350	6.12	41710	22.8	1.76×10^{-5}
-69° 104	O6 Ib(f)	2500	6.08	41710	21.8	8.22×10^{-6}
-66° 100	O6 II(f)	2075	5.64	42000	13.0	2.02×10^{-6}
-70° 91	O6.5 V	3150	5.81	42280	15.6	2.48×10^{-6}
-67° 111	O7 Ib(f)	2000	5.82	38720	18.8	3.71×10^{-6}

1) $\log L/L_\odot$ using $DM_{LMC} = 18.30$ (Fitzpatrick et al. (2001) and Vacca et al. T_{eff} calibration.

2) T_{eff} from the Vacca, Garmany & Shull (1996) calibration.

3) \dot{M} from the Vink, de Koter & Lammers (2001) relationship.

Table 2: Ion Fractions

$\chi_{i-1} - \chi_i$	24–48	30–47	33–45	35–47	48–64	51–65	73–88	77–98	114–138
Sanduleak	C III	N III	Si IV	S IV	C IV	P V	S VI	N V	O VI
-67° 211	–	–	–	–	5.7×10^{-4}	–	1.4×10^{-3}	5.5×10^{-2}	5.4×10^{-3}
-66° 172	–	–	–	–	5.9×10^{-4}	–	2.9×10^{-3}	2.0×10^{-2}	1.4×10^{-3}
-67° 166	2.2×10^{-5}	2.9×10^{-3}	3.9×10^{-4}	2.6×10^{-3}	4.0×10^{-4}	4.2×10^{-2}	2.1×10^{-3}	3.9×10^{-3}	9.5×10^{-5}
-67° 167	1.2×10^{-4}	1.5×10^{-3}	4.6×10^{-4}	3.5×10^{-3}	1.2×10^{-3}	5.0×10^{-2}	2.6×10^{-3}	7.0×10^{-3}	1.0×10^{-3}
-70° 115	6.3×10^{-5}	3.8×10^{-3}	×	–	×	8.4×10^{-3}	7.2×10^{-4}	×	2.2×10^{-4}
-71° 45	–	–	1.7×10^{-4}	–	9.1×10^{-4}	–	8.3×10^{-4}	5.4×10^{-3}	3.1×10^{-4}
-70° 60	–	–	–	–	1.5×10^{-3}	–	1.7×10^{-2}	1.0×10^{-2}	1.9×10^{-3}
-70° 69	–	–	–	–	3.0×10^{-3}	–	3.1×10^{-2}	3.5×10^{-2}	2.2×10^{-2}
-65° 22	9.3×10^{-5}	7.0×10^{-3}	2.7×10^{-3}	1.3×10^{-2}	7.1×10^{-4}	3.8×10^{-2}	1.1×10^{-3}	4.3×10^{-3}	4.2×10^{-5}
-69° 104	1.7×10^{-4}	2.1×10^{-3}	7.9×10^{-4}	–	2.1×10^{-3}	4.5×10^{-2}	2.8×10^{-3}	3.1×10^{-3}	9.7×10^{-4}
-66° 100	1.3×10^{-4}	4.1×10^{-3}	–	–	4.1×10^{-3}	1.0×10^{-1}	4.8×10^{-3}	1.6×10^{-2}	1.0×10^{-3}
-70° 91	–	–	–	–	9.2×10^{-4}	–	9.9×10^{-3}	1.2×10^{-2}	3.0×10^{-3}
-67° 111	5.9×10^{-4}	1.7×10^{-2}	2.4×10^{-3}	2.3×10^{-2}	1.6×10^{-3}	1.4×10^{-1}	1.3×10^{-2}	1.1×10^{-2}	1.3×10^{-3}

1) Assuming $A_E(\text{LMC}) = 0.6A_E(\text{Galactic})$ for all species.

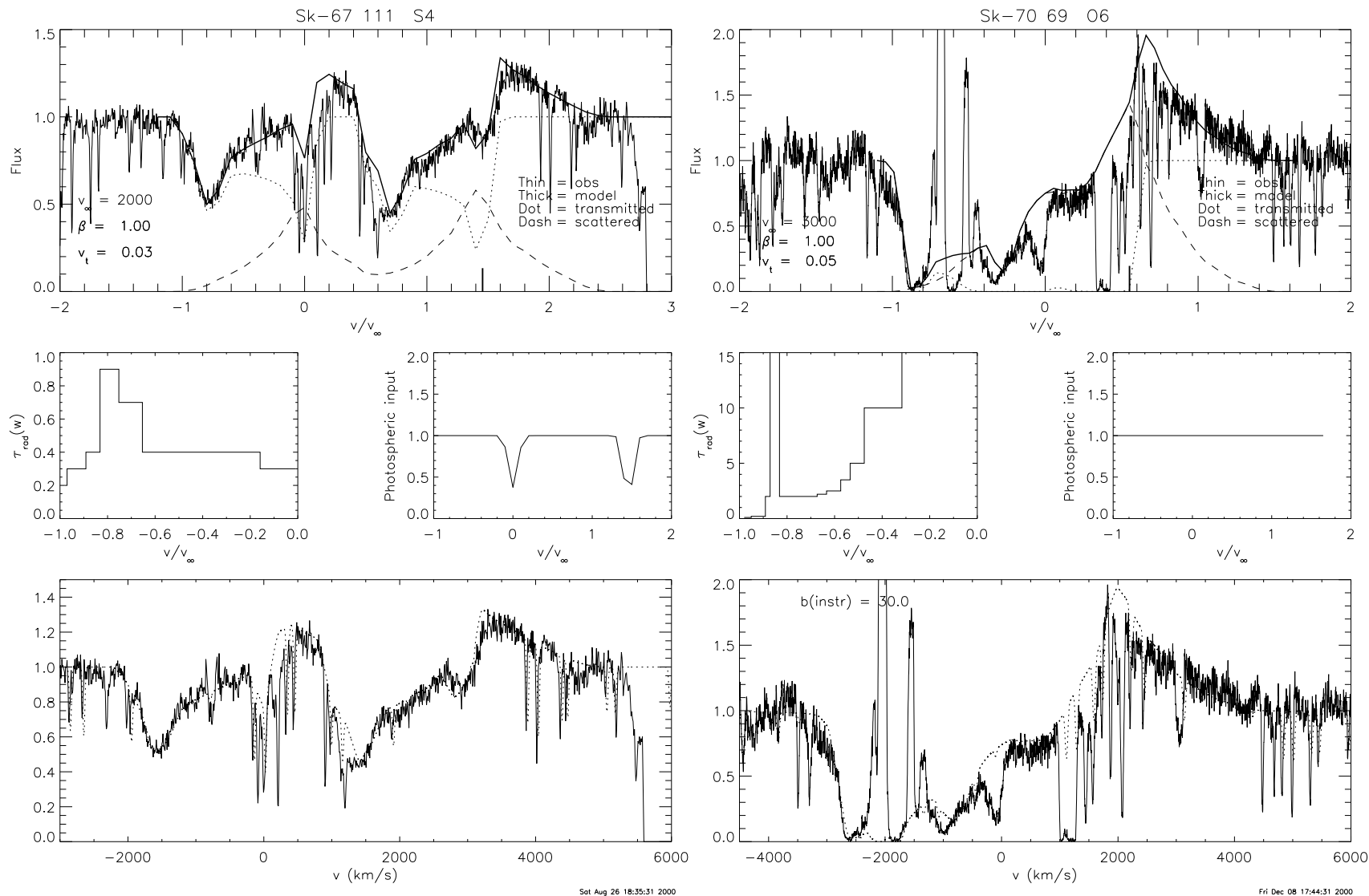


Figure 1: Examples of fits for S IV in Sk-67° 111 (left) and O VI in Sk-70° 69 (right). The velocity scales are in the rest frame of the stars. In each plot, the *top panel* shows the raw model output, the observed spectrum, and the contributions to the model profile from transmitted and scattered light. A thick tick mark denotes the rest position of the red component of the doublet. The *middle panels* show τ_{rad} and the input photospheric profile as a function of v/v_∞ . The *bottom panel* compares the observed profile to the model model once an H I + H₂ ISM model has been applied to the model and the result convolved with the instrumental profile.

Figure 2 – part 1

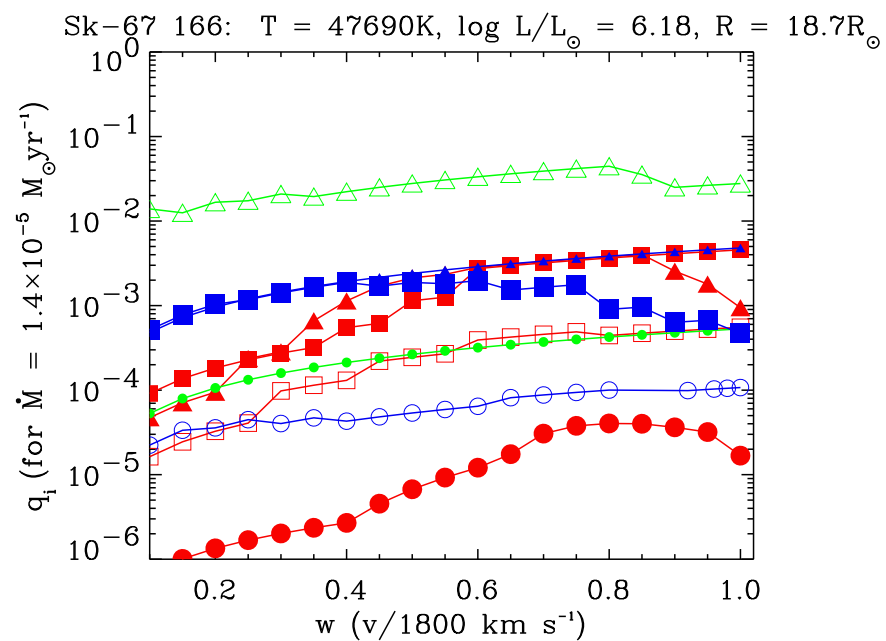
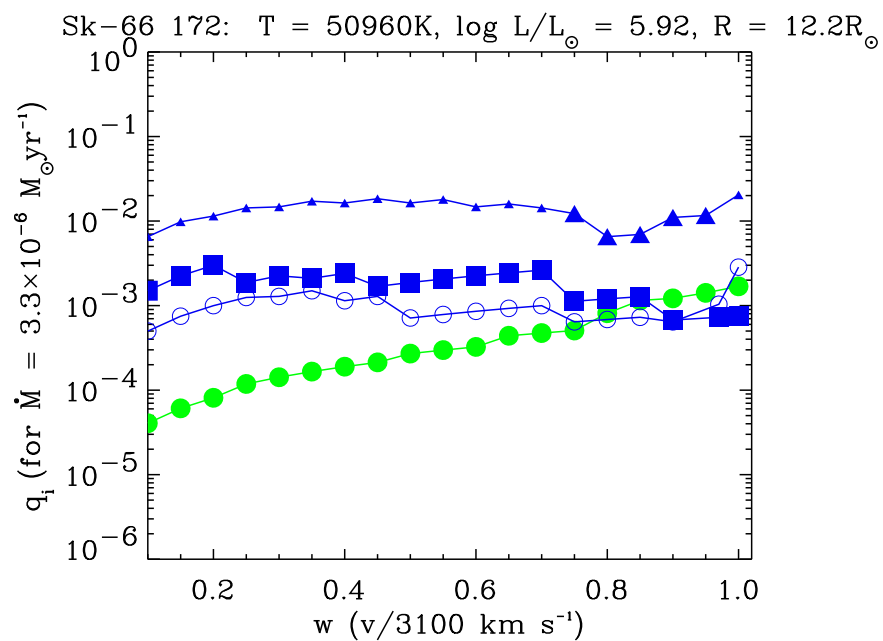
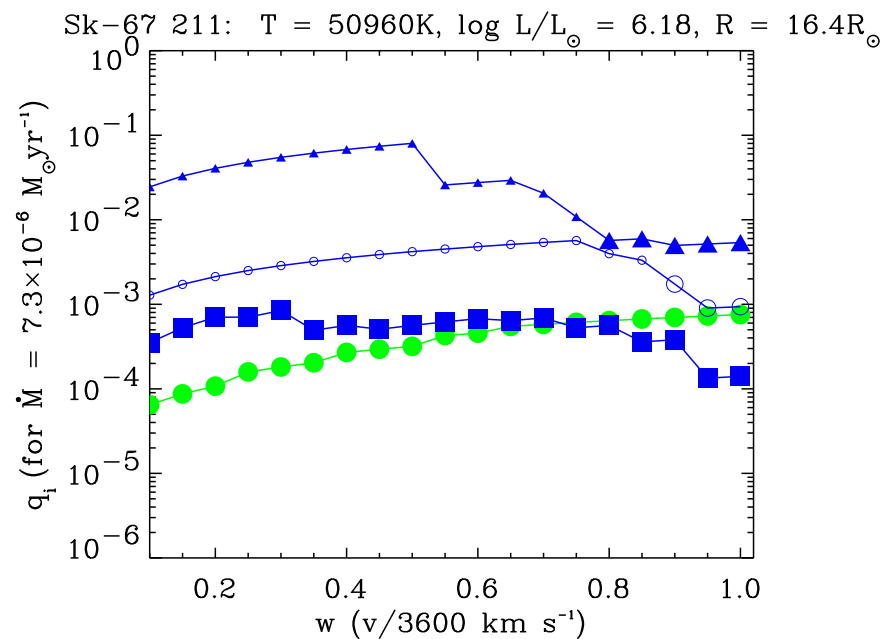
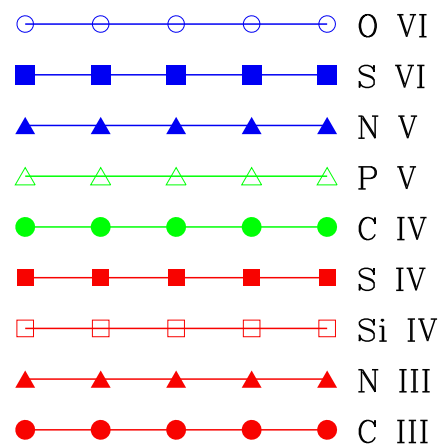


Figure 2 – part 2

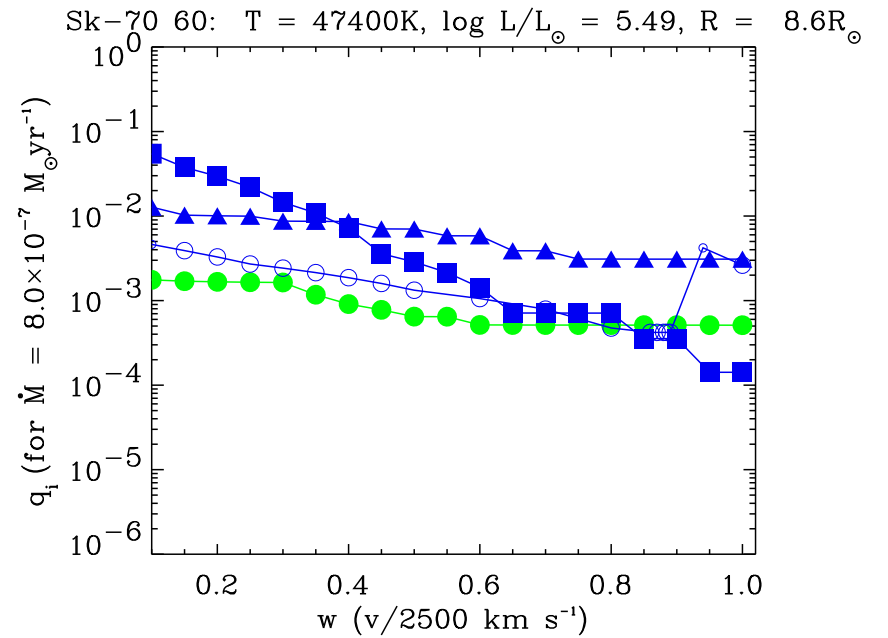
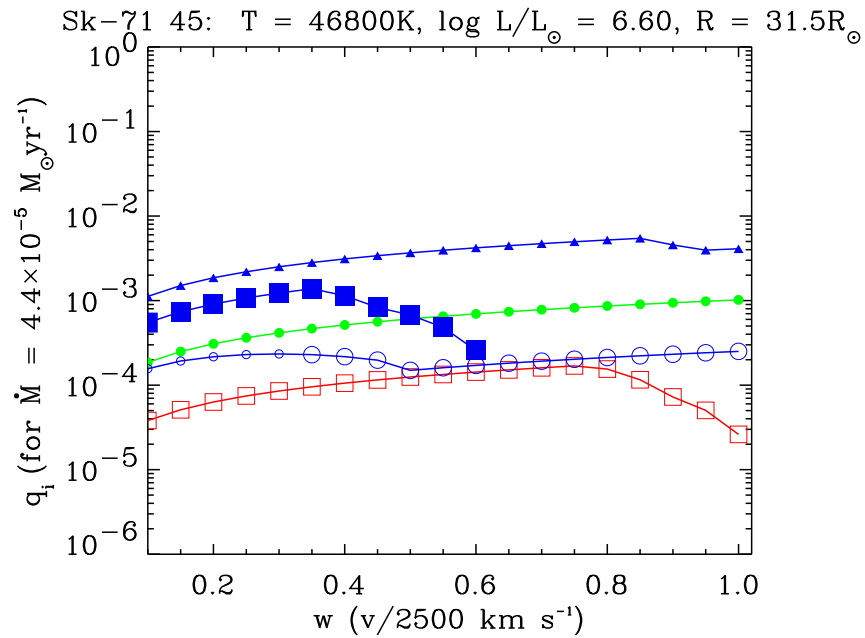
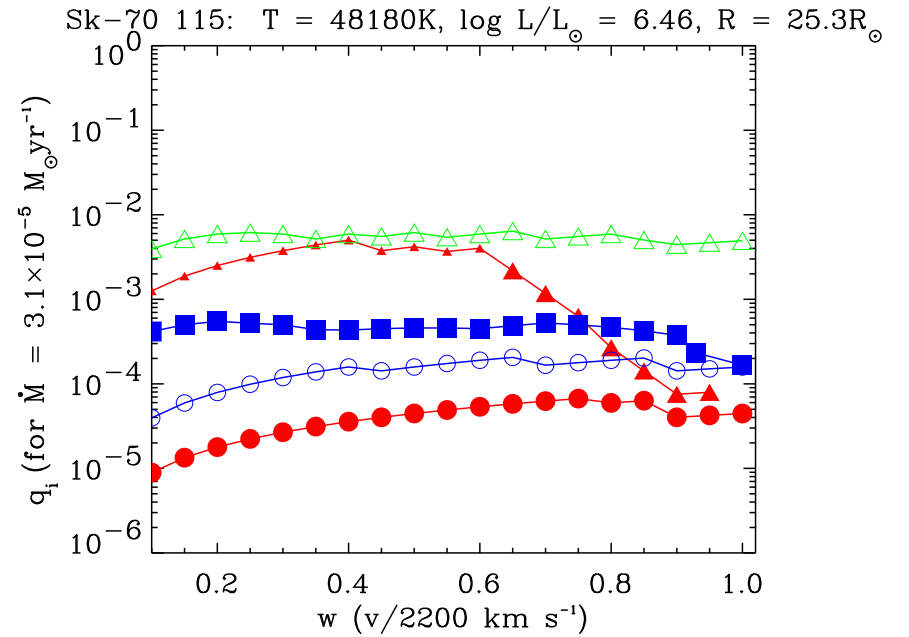
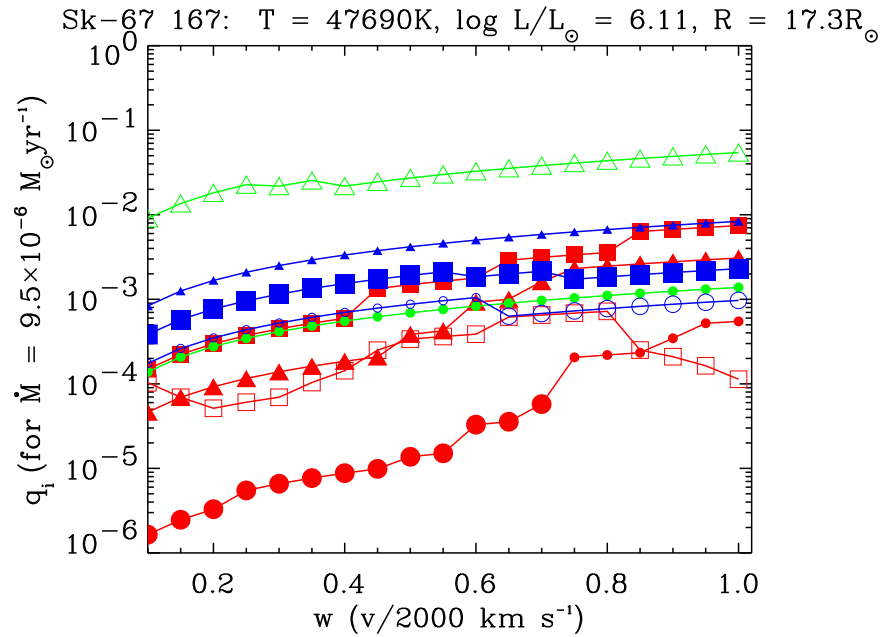


Figure 2 – part 3

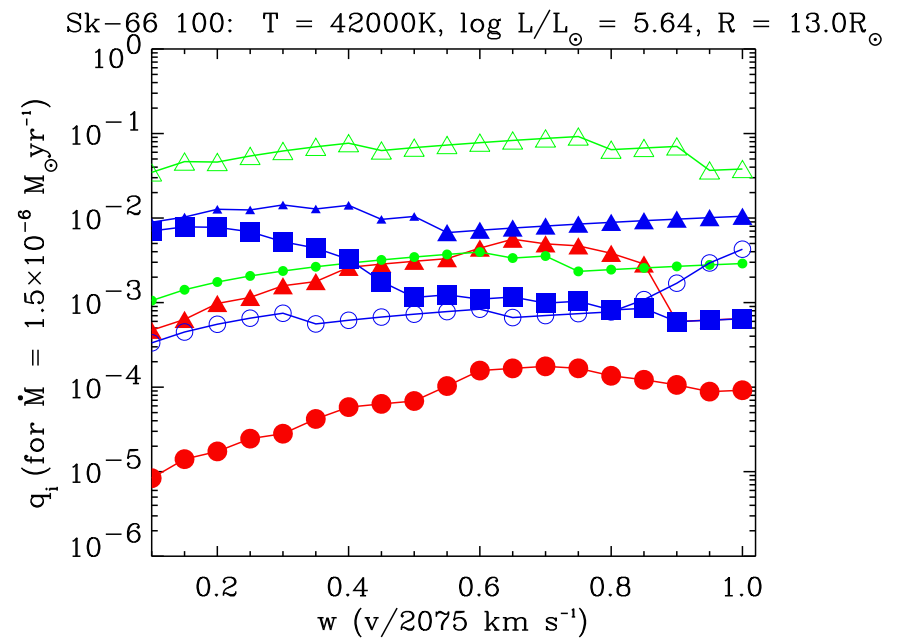
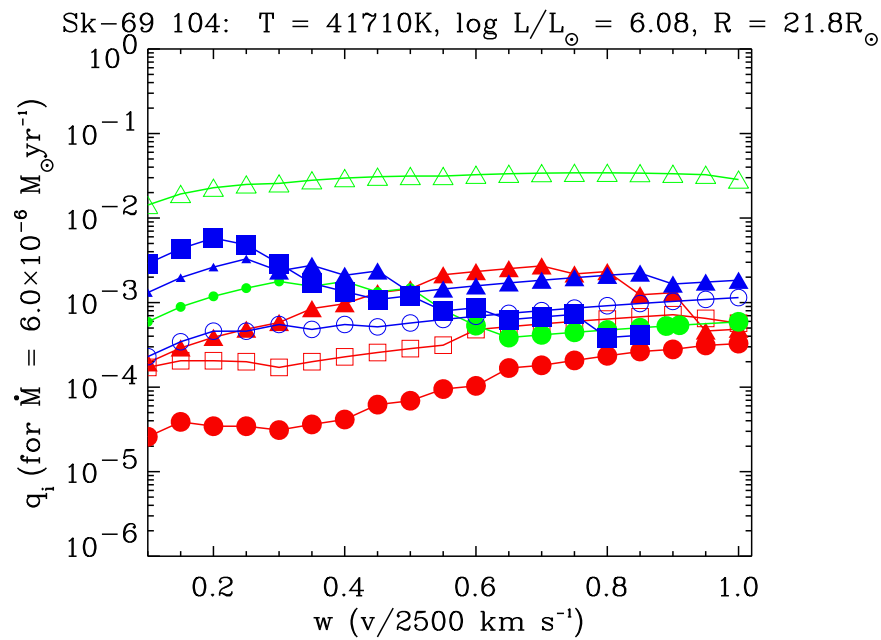
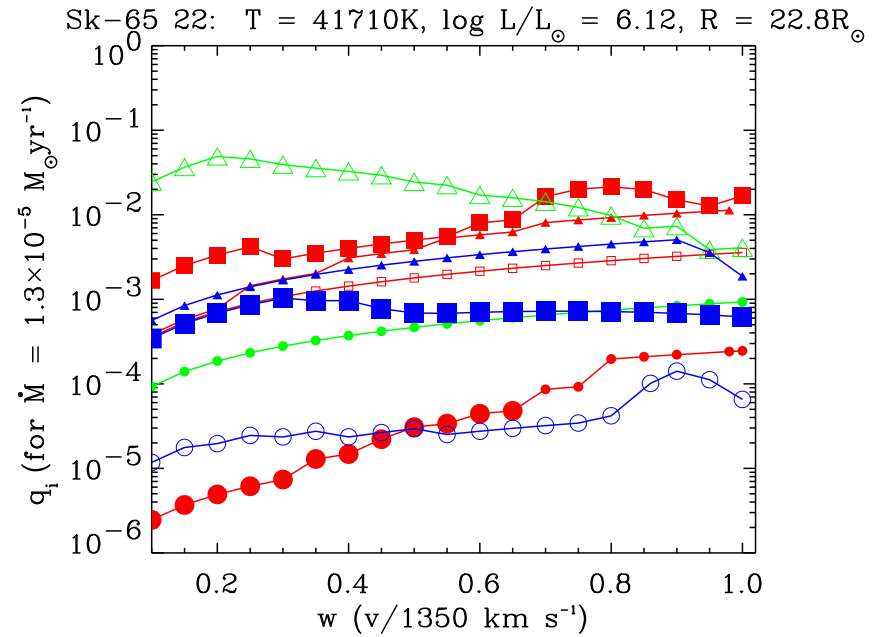
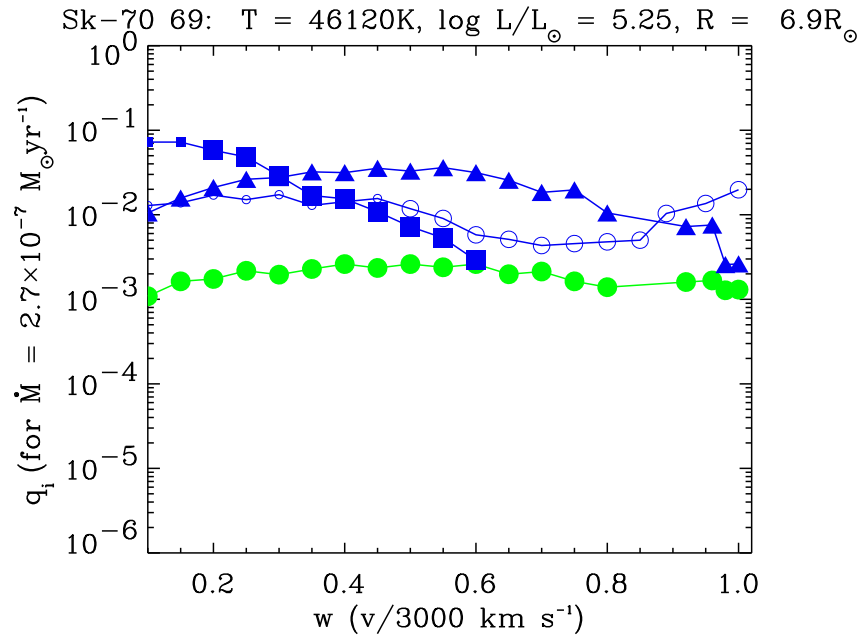


Figure 2 – part 4

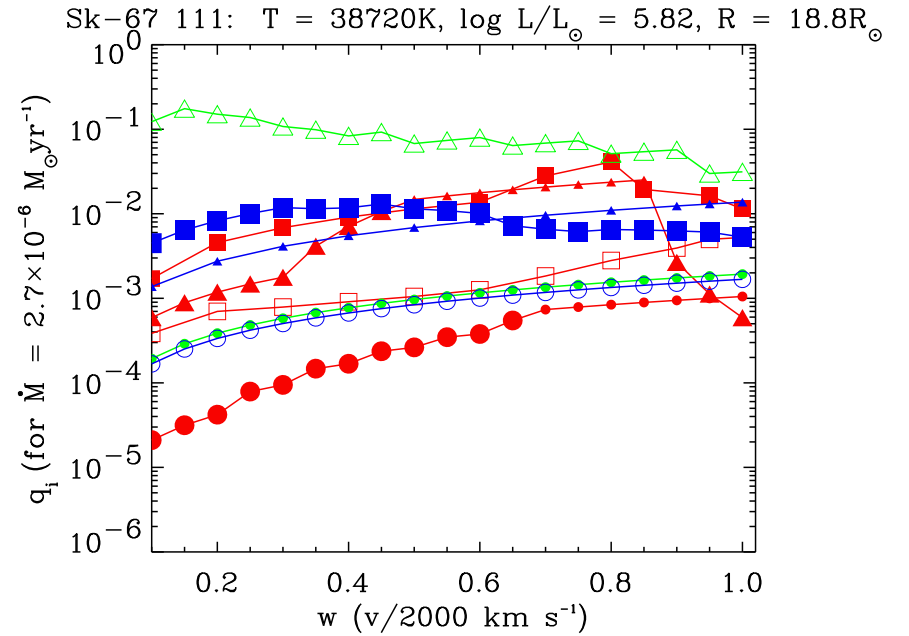
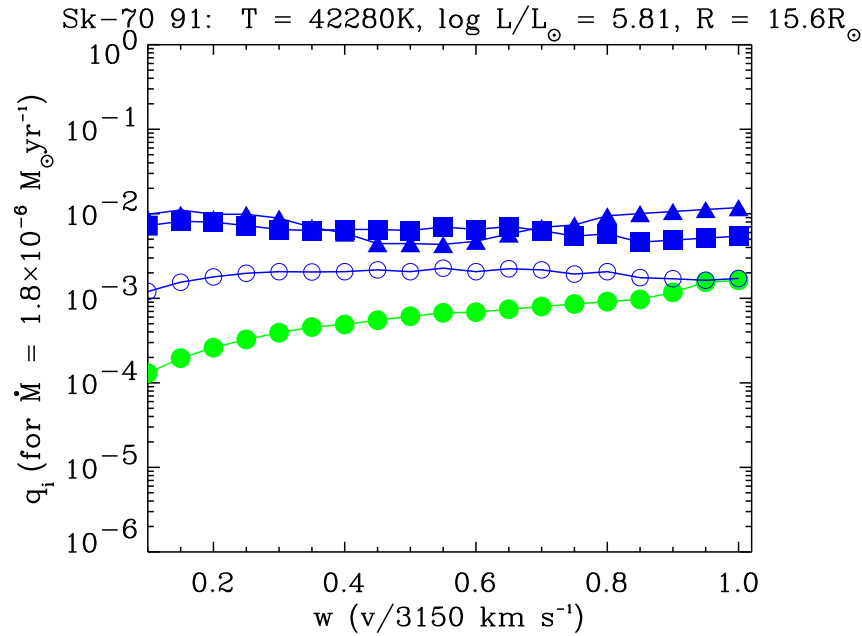


Figure 2: Ion fractions, q_i , as a function of $w = v/v_{\infty}$, for each program star. The values of \dot{M} listed in Table 1 were used and the LMC abundances were set to $0.6 \times \text{Galactic}$ for all species. The key for the different symbols and colors is given in the first panel. Ion fractions determined from saturated τ_{rad} bins ($\tau_{rad} > 4$ for a singlet or 8 for a doublet) are shown as small symbols.

Figure 3 – part 1

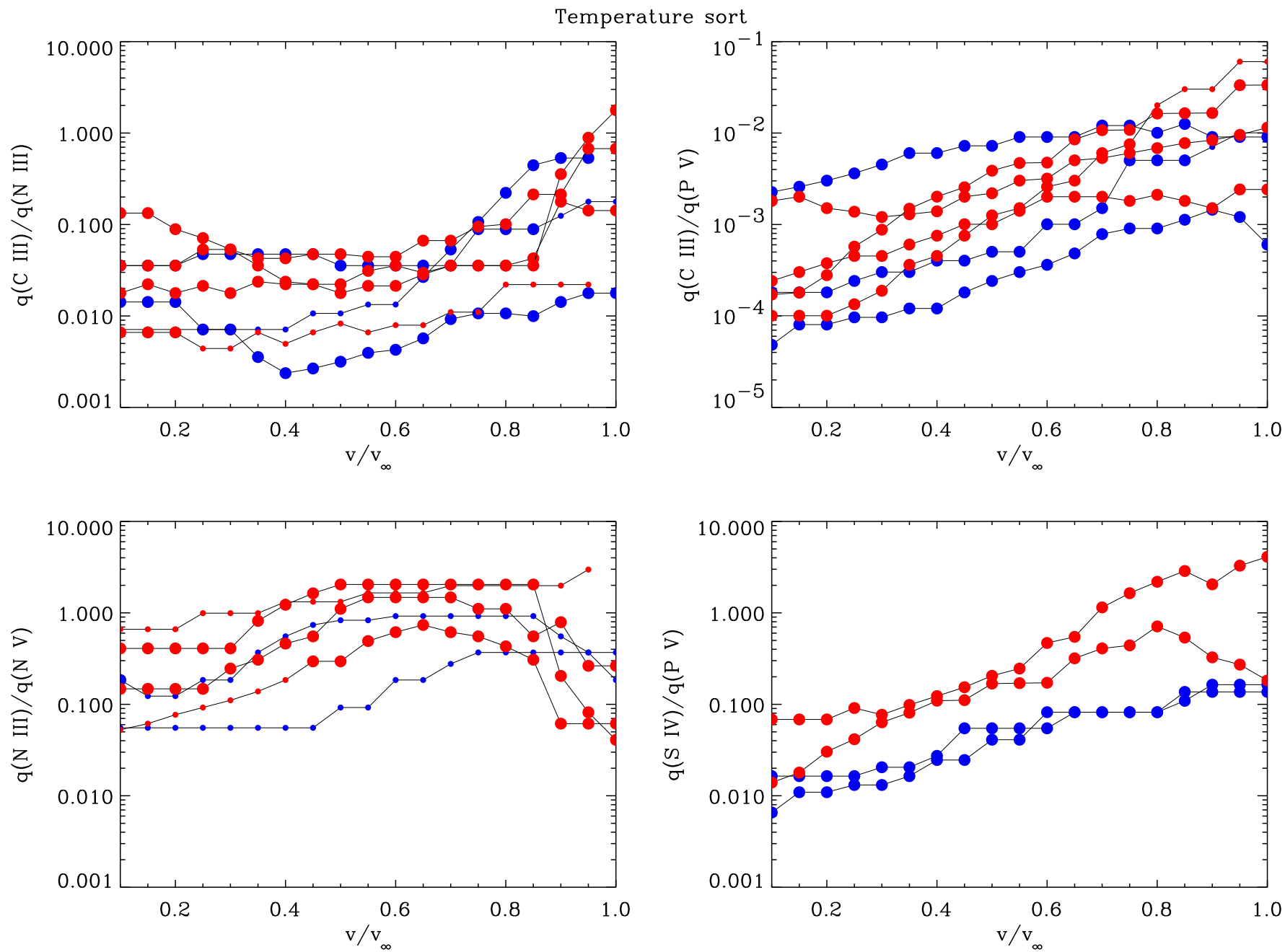


Figure 3 – part 2

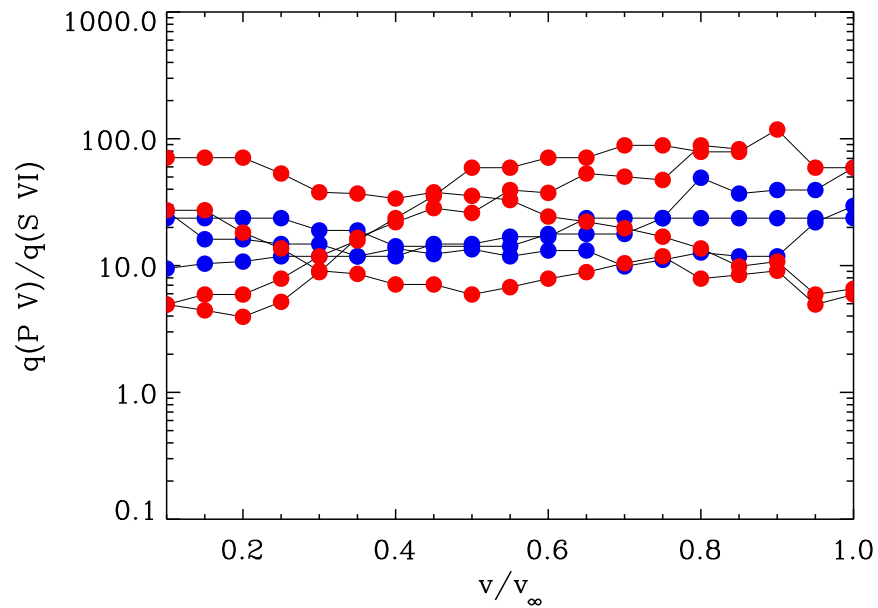
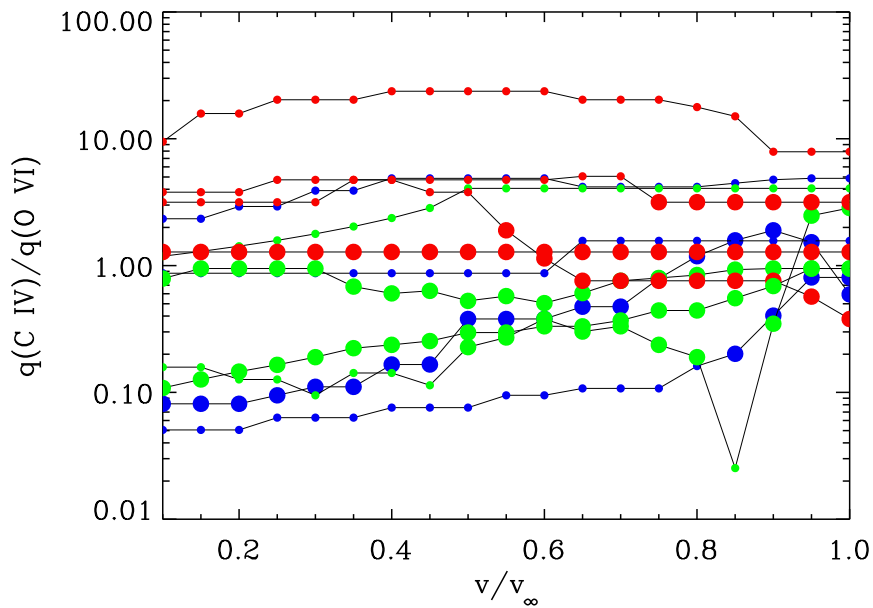
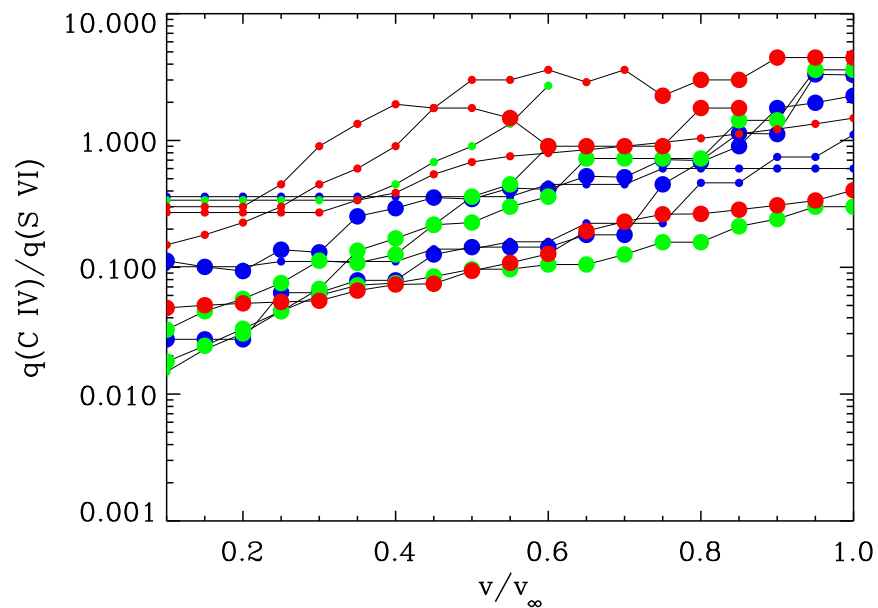
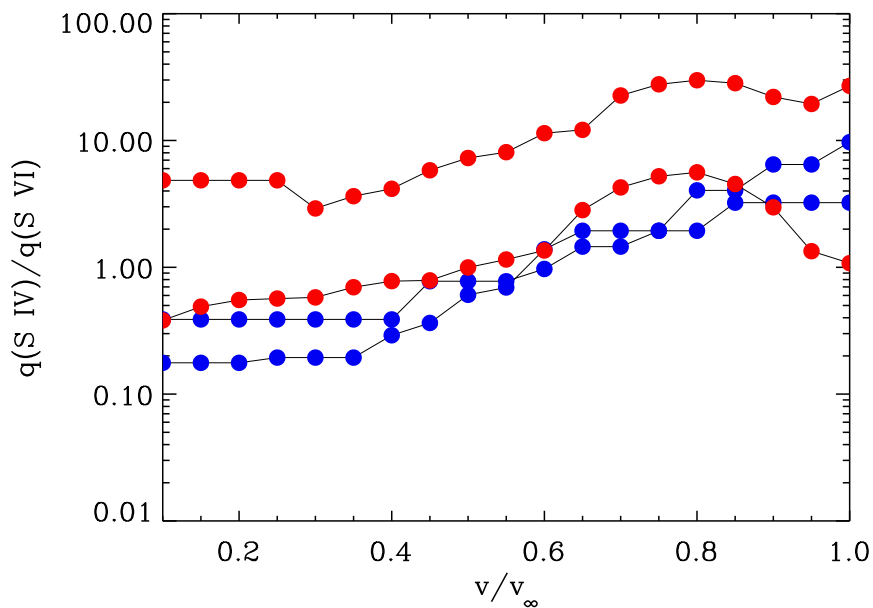


Figure 3 – part 3

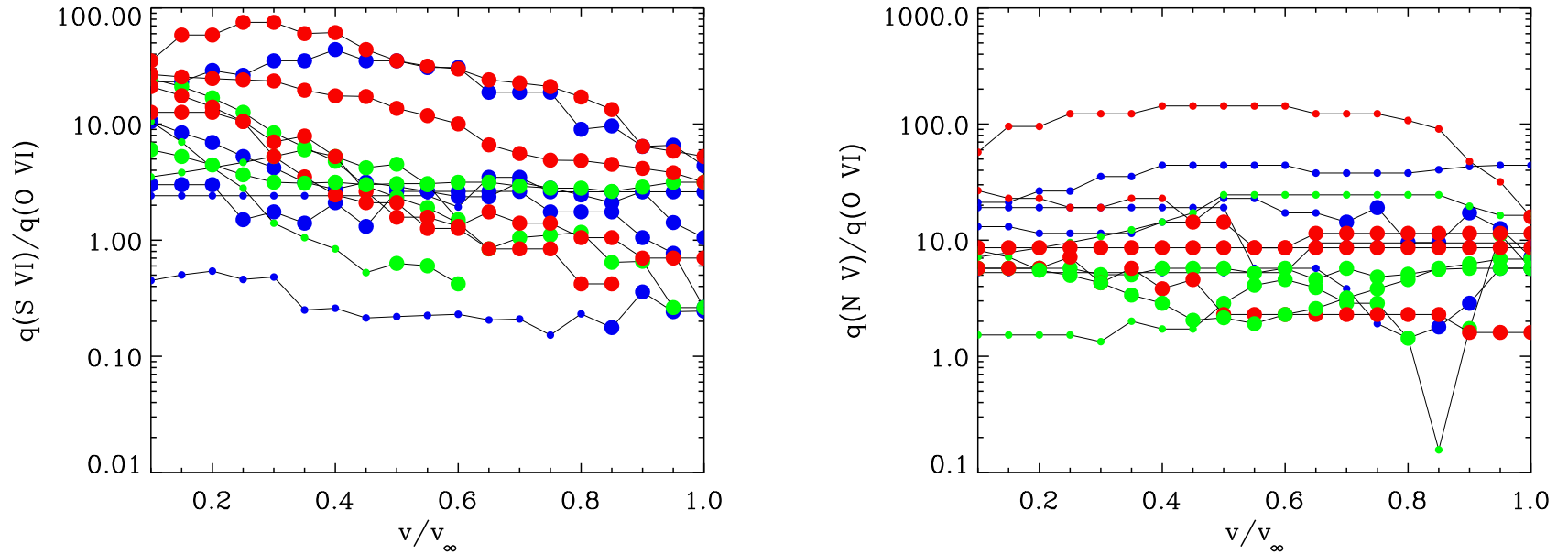


Figure 3: Examples of ion ratios as a function of $w = v/v_\infty$. These quantities do not depend on the \dot{M} estimates, but are affected by abundance anomalies. As in Fig. 2, ratios determined from saturated τ_{rad} bins in *either* species are shown as small symbols. The different colors are for different temperatures, with *red* for $T_{eff} \leq 42000$ K, *green* for $42000 < T_{eff} \leq 47500$ K, and *blue* for $47500 < T_{eff}$. When examining all such figures, several interesting trends emerge:

1. Lower ions usually increase relative to high ions as w increases, but O VI does not follow this trend.
2. Often, the w dependence of the low-to-high ion ratio is steeper for cooler stars.
3. In contrast to ratios containing CNO ions, ratios of *non*-CNO ions have smaller dispersions and tend to be T_{eff} ordered, with cooler stars having relatively more of the lower ions.
4. While the non-CNO ratios for Sk-67°166 and Sk-67°167 are nearly identical, their CNO to non-CNO ratios are highly disparate, with Sk-67°166 having far more N and much less C, revealing a strong CNO anomaly in this star.

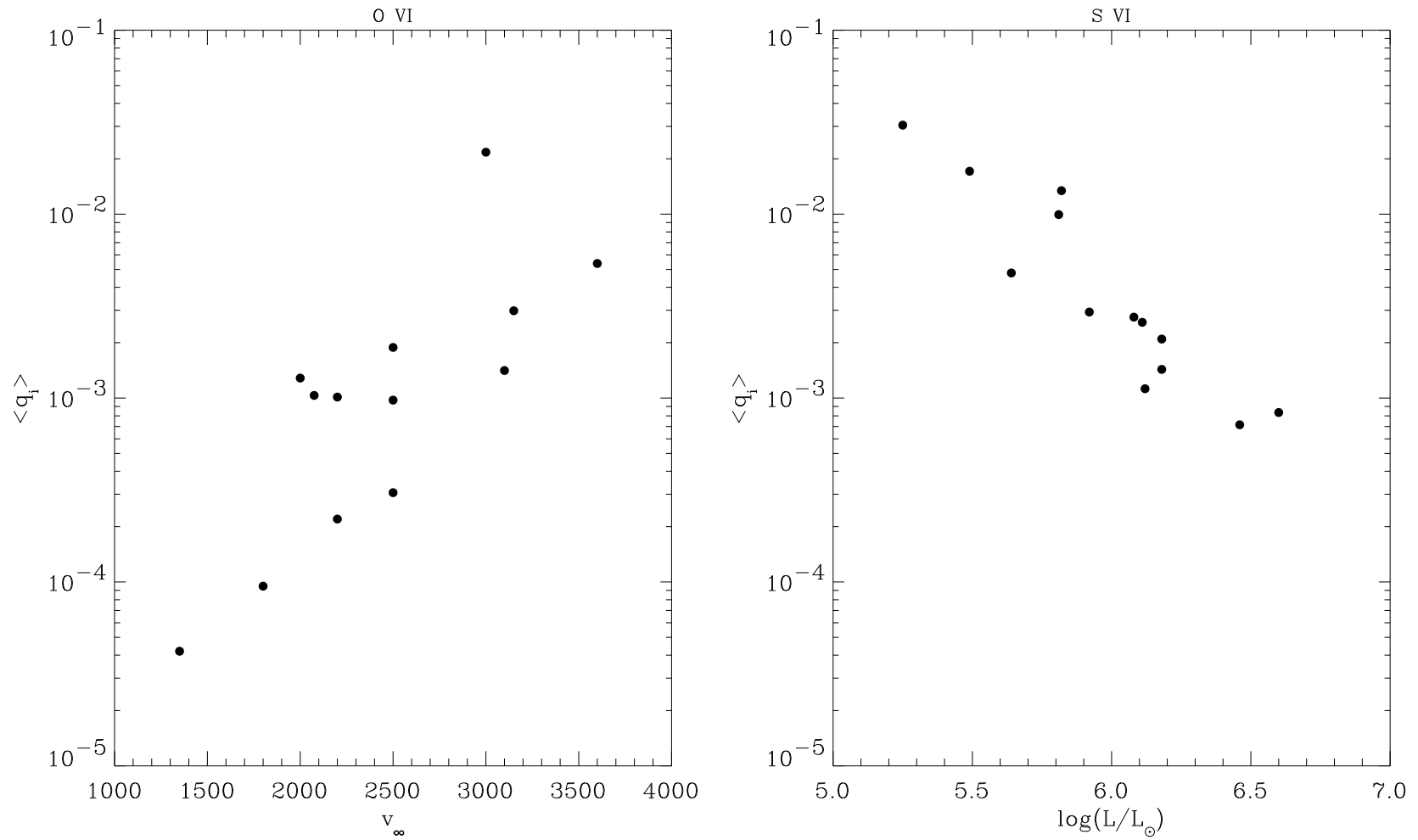


Figure 4: Correlations between the mean ion fraction (integrated over $0.2 < w < 0.9$) of O VI and v_∞ (left) and S VI and $\log L/L_\odot$ (right). These are the only strong correlations between ion fractions and stellar parameters.